Areas of superconductivity and giant proximity effects in underdoped cuprates

Gonzalo Alvarez,[1] Matthias Mayr,[2] Adriana Moreo,[1] and Elbio Dagotto[1]
[1]*National High Magnetic Field Lab and Department of Physics, Florida State University, Tallahassee, Florida 32310, USA*
[2]*Max-Planck-Institut für Festkörperforschung, 70569 Stuttgart, Germany*
(Received 16 January 2004; revised manuscript received 14 October 2004; published 20 January 2005)

Phenomenological models for the antiferromagnetic (AF) versus *d*-wave superconductivity competition in cuprates are studied using conventional Monte Carlo techniques. The analysis suggests that cuprates may show a variety of different behaviors in the very underdoped regime: local coexistence or first-order transitions among the competing orders, stripes, or glassy states with nanoscale superconducting (SC) puddles. The transition from AF to SC does not seem universal. In particular, the glassy state leads to the possibility of "colossal" effects in some cuprates, analog of those in manganites. Under suitable conditions, nonsuperconducting Cu-oxides could rapidly become superconducting by the influence of weak perturbations that align the randomly oriented phases of the SC puddles in the mixed state. Consequences of these ideas for thin-film and photoemission experiments are discussed.

DOI: 10.1103/PhysRevB.71.014514 PACS number(s): 74.20.De, 74.20.Rp, 74.72.−h

I. INTRODUCTION

Clarifying the physics of high-temperature superconductors (HTS) is still one of the most important challenges in condensed-matter physics. There is overwhelming experimental evidence for several unconventional regimes in HTS, including a pseudogap region at temperatures above the superconducting (SC) phase and a largely unexplored glassy state separating the parent antiferromagnet (AF) from the SC phase at low hole-doping x. In addition, recent investigations unveiled another remarkable property of HTSs that defies conventional wisdom: the existence of *giant proximity effects* (GPE) in some cuprates,[1–3] where a supercurrent in Josephson junctions was found to run through non-SC Cu-oxide-based thick barriers. This contradicts the expected exponential suppression of supercurrents with barrier thickness beyond the short coherence length of Cu-oxides. The purpose of this paper is to propose an explanation based on a description of the glassy state as containing SC *puddles*. This nanoscale inhomogeneous state leads to *colossal effects in cuprates*, in analogy with manganites.[4–6] In addition, it is argued that different inhomogeneous states could be stabilized in different Cu-oxides, depending on coupling and quenched disorder strengths. In fact, neutron-scattering studies have revealed "stripes" of charge in Nd-LSCO,[7,8] but scanning tunneling microscopy (STM) experiments[9,10] indicate "patches" in Bi2212, consistent with our analysis. There is no unique way to transition from AF to SC.

Studies of the *t-J* model have revealed SC and striped states[11,12] evolving from the undoped limit. Then, it is reasonable to assume that AF, SC, and striped states are dominant in cuprates, and their competition regulates the HTS phenomenology. However, further computational progress using basic models is limited by cluster sizes that cannot handle the nanoscale structure unveiled by STM experiments. Considering these restrictions, here a *phenomenological* approach will be pursued to understand how these phases compete, incorporating the quenched disorder inevitably introduced by chemical doping. This effort unveils effects of experimental relevance not captured with first-principles studies. Two models are used, one with itinerant fermions and the other without, and the conclusions are similar in both. Hopefully, this effort will jump-start a more detailed computational analysis of phenomenological models in the high-Tc arena, since most basic first-principles approaches, including Hubbard and *t-J* investigations, have basically reached their limits, particularly regarding cluster sizes that can be studied.

II. MODEL I: ITINERANT FERMIONS

The analysis starts with a phenomenological model of itinerant electrons (simulating carriers) on a square lattice, locally coupled to classical order parameters

$$H_F = -t\sum_{\langle \mathbf{ij}\rangle,\sigma}(c^\dagger_{\mathbf{i}\sigma}c_{\mathbf{j}\sigma}+\text{H.c.}) + 2\sum_{\mathbf{i}} J_{\mathbf{i}} S^z_{\mathbf{i}} s^z_{\mathbf{i}} - \sum_{\mathbf{i}\sigma}\mu_{\mathbf{i}} n_{\mathbf{i}\sigma} + \frac{1}{D}\sum_{\mathbf{i},\alpha}\frac{1}{V_{\mathbf{i}}}|\Delta_{\mathbf{i}\alpha}|^2 - \sum_{\mathbf{i},\alpha}(\Delta_{\mathbf{i}\alpha}c_{\mathbf{i}\uparrow}c_{\mathbf{i}+\alpha\downarrow}+\text{H.c.}), \quad (1)$$

where $c_{\mathbf{i}\sigma}$ are fermionic operators, $s^z_{\mathbf{i}}=(n_{\mathbf{i}\uparrow}-n_{\mathbf{i}\downarrow})/2$, $n_{\mathbf{i}\sigma}$ is the number operator, D is the lattice dimension, and $\Delta_{\mathbf{i}\alpha}=|\Delta_{\mathbf{i}\alpha}|e^{i\phi^\alpha_{\mathbf{i}}}$ are complex numbers for the SC order parameter defined at the links $(\mathbf{i},\mathbf{i}+\alpha)$ (α=unit vector along the x or y directions). At $J_{\mathbf{i}}=0$, *d*-wave SC is favored close to half filling because the pairing term involves nearest-neighbor sites, as in any standard mean-field approximation to SC. The spin degrees of freedom (DOF) are assumed to be Ising spins (denoted by $S^z_{\mathbf{i}}$). Studies with O(3) DOF were found to lead to qualitatively similar conclusions, but they are more CPU time consuming. The parameters of relevance are $J_{\mathbf{i}}$, $\mu_{\mathbf{i}}$, and $V_{\mathbf{i}}$ (t is the energy unit), that carry a site dependence to easily include quenched disorder, which is inevitable in chemically doped compounds as the cuprates. For a fixed configuration, $\{\Delta_{\mathbf{i}\alpha}\}$ and $\{S^z_{\mathbf{i}}\}$, the one-particle sector is Bogoliubov diagonalized. In the limit $T\to 0$, the Bogoliubov–de Gennes equations are recovered minimizing the energy.[13–15] Then, a standard Monte Carlo (MC) simulation similar to those for

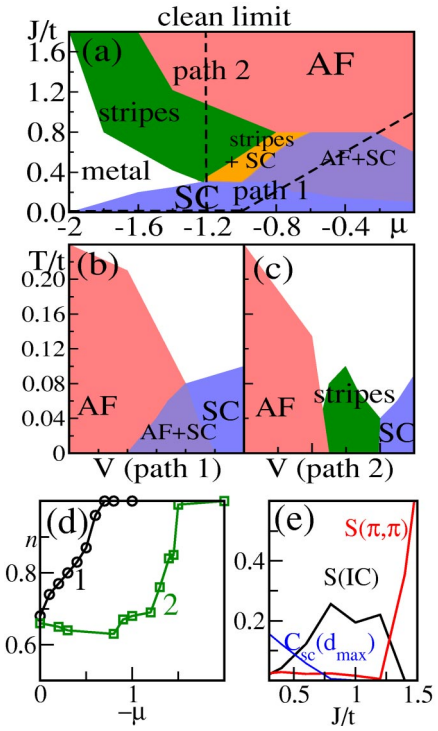

FIG. 1. (Color online) (a) MC phase diagram for Eq. (1) without disorder at low temperatures. Instead of presenting a three-dimensional phase diagram we have chosen to present a two-dimensional cut along $V=1-J/2$ for simplicity. Five regions are observed: AF, *d*-SC, stripes, coexisting SC+AF, coexisting stripes +SC, and metallic. (b) MC phase diagram including temperature along path 1. (c) MC phase diagram along path 2. Lattice sizes in all cases are 8×8 and 12×12. (d) n vs μ along Paths 1 and 2. Transitions along Path 1 appear continuous, whereas along path 2 there are indications of first-order transitions. (e) Spin structure factor $S(\mathbf{q})$ at (π,π) and for incommensurate (IC) momenta.

Kondo-lattice models is carried out (details in Ref. 4). One of the goals is to estimate T_c, as well as T_c^*, roughly defined as the temperature at which strong short-distance SC correlations develop (more details are given below). Finally, note that model Eq. (1) is not derived but *proposed* as a possible phenomenological model for AF versus SC competition. The results will be shown to justify this assumption. Moreover, the qualitative simplicity of our conclusions suggests that similar models will lead to similar scenarios.

A. Phase diagram in the clean limit

Without quenched disorder, $V_\mathbf{i}$, $J_\mathbf{i}$, and $\mu_\mathbf{i}$ in Eq. (1) are site independent. The standard MC analysis carried out in these investigations (details provided below) reveals that in the clean limit the low-temperature (T) phase diagram [Fig. 1(a)] has a robust AF phase for electronic densities $n\sim1$ and a *d*-wave SC phase for $n<1$. The *d*-wave correlation function, defined as

$$C_{sc}^{\alpha\beta}(\mathbf{m}) = \sum_\mathbf{i} \langle |\Delta_\mathbf{i}||\Delta_{\mathbf{i}+\mathbf{m}}|\cos(\phi_\mathbf{i}^\alpha - \phi_{\mathbf{i}+\mathbf{m}}^\beta)\rangle, \qquad (2)$$

was used to estimate T_c as the temperature at which *d*-wave correlations at the largest distances for the lattices considered here are 5% of their maximum value at $|\mathbf{m}|=0$. The 5% criterion is arbitrary but other criteria lead to identical qualitative trends, slightly shifting the phase diagrams. T^* is deduced similarly, but using the shortest nonzero distance correlation function ($|\mathbf{m}|=1$). The Néel temperature T_N associated with the classical spins was defined by the drastic reduction ($\leqslant5\%$ of $|\mathbf{m}|=0$ value) of the long-distance spin order using $C_S(\mathbf{m})=\Sigma_\mathbf{i}\langle S_\mathbf{i}^z S_{\mathbf{i}+\mathbf{m}}^z\rangle$, while T_N^* relates to short-range spin order. The results presented in Fig. 1(a) are not surprising because these states are favored explicitly in Eq. (1) by the second and fifth terms, respectively. However, the phase diagram presents several nontrivial interesting regions: (i) Along path 1 in Fig. 1(a), the AF-SC transition occurs through *local* coexistence, with tetracritical behavior [Fig. 1(b)].[16] (ii) Along path 2 the AF-SC interpolating regime has alternating doped and undoped *stripes* (stripes in MC data are deduced from spin and charge structure factors, and low-T MC snapshots), and a complex phase diagram [Fig. 1(c)]. These stripes evolve continuously from the $V=0$ limit that was studied before by Moraghebi *et al.*, and, as a consequence, we refer the readers to Ref. 17 for further details on how stripes were identified. It remains to be investigated to see if these stripes, involving SC and AF quasi-1D lines, have the same or different origin as those widely discussed before in the high-Tc literature.[12,18–22] At $V\neq0$, the doped regions of the stripes have nonzero SC amplitude at the mean-field level.[23] In view of the dramatically different behavior along paths 1 and 2, we conclude that in our model *there is no unique AF→SC path*. This is in agreement with experiments, as $La_{2-x}Sr_xCuO_4$ (LSCO) and others have stripes,[7,8,24] while $Ca_{2-x}Na_xCuO_2Cl_2$ has a more complex inhomogeneous pattern.[10] Both, however, become SC with increasing x. This suggests that *the underdoped region of Cu-oxides may not be universal*.

B. Phase diagram with quenched disorder

Our results become even more interesting upon introducing quenched disorder, with a MC phase diagram shown in Fig. 2(b). The similarity with the widely accepted phase diagram of the cuprates is clear. The disorder has opened a hole-density "window" where none of the two competing orders dominates. Inspecting "by eye" the dominant MC configurations (snapshots) at low T in this intermediate regime reveals a patchy system with slowly evolving islands of SC or AF and random orientations of the local-order parameters, leading to an overall disordered "clustered" state. In Fig. 2(b), a temperature scale T^* at which the fermionic density-of-states (DOS) develops a *pseudogap* (PG) [Fig. 2(c)] was also presented. The AF and *d*-SC regions both have a gap (smeared by T and disorder, but, nevertheless, with recognizable features). But even the "disorder" regime [case b in Fig. 2(c)] has a PG. MC snapshots explains this behavior: in the disordered state there are small SC or AF regions, as explained above. Locally each has a smeared-gap DOS, either AF or SC. Not surprisingly, the mixture presents a PG. The behavior of T^* versus x is remarkably similar to that found experimentally. The *cuprates' PG may arise from an overall-disordered clustered state with local* AF *or* SC *ten-*

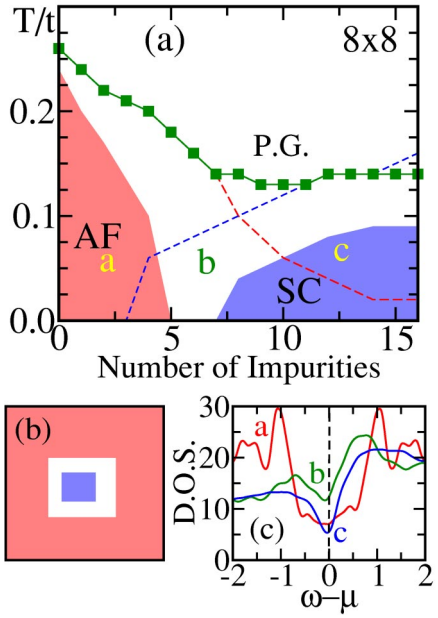

FIG. 2. (Color online) (a,b) Plaquette impurity schematic representation. Disorder may have several forms, but here we mimic Sr doping in single layers. Sr^{2+} replaces La^{3+} above the center of a Cu-plaquette in the Cu-oxide square lattice. Then, as hole carriers are added, a hole-attractive plaquette-centered potential should also be incorporated. Near the center of this potential, n should be sufficiently reduced from 1 that, phenomenologically, tendencies to SC should be expected. To interpolate between the SC central plaquette and the AF background, a plaquette "halo" with no dominant tendency was introduced. Parameters are chosen such that the blue (black) region favors superconductivity, $(J,V,\mu)=(0.1,1.0,-1.0)$, with a surrounding white region where $(J,V,\mu)=(0.1,0.1,-0.5)$ with no order prevailing. The impurity is embedded in a background (red and dark gray), which favors the AF state, $(J,V,\mu)=(1.0,0.1,0.0)$. However, the overall conclusions found here are simple and independent of the disorder details. MC phase diagram for model Eq. (1), including quenched disorder (lattices studies are 8×8 (results shown) and 12×12). Shown are T_c and T_N vs number of impurities (equal to number of holes). The SC and AF regions with short-range order (dashed lines) and T^* as obtained from the PG (dot-dashed line) are also indicated. (c) DOS at points *a*, *b*, and *c* of (a), with a PG.

dencies, without the need to invoke other exotic states. This PG is correlated with robust short-range correlations [dashed lines in Fig. 2(b), see caption for details].

The numerical procedure that led to Figs. 1 and 2 is standard, well known in the manganite context where formally similar models are widely studied,[4–6] thus, here only a few representative results will be presented for completeness. For instance, Fig. 3(a) shows the order parameters along path 1 of Fig. 1(a), indicating how each ordered region was determined in the clean limit. Clearly, a region of coexistence can be observed. Similar data were used to complete the phase diagram. Likewise, Fig. 3(b) contains the order parameter versus T with and without disorder, in the interesting region of couplings and doping. There is a drastic difference between clean and dirty limits, the latter showing no global dominant order. However, examining relevant MC configurations, small SC and AF clusters with random orientations are found.

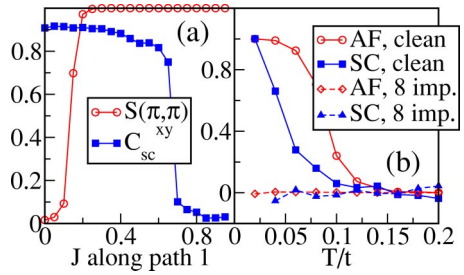

FIG. 3. (Color online) (a) MC $S(\pi,\pi)$ and superconducting correlation at maximum distance C_{sc}^{xy} [Eq. (2)] along path 1 [Fig. 1(a)], using an 8×8 lattice and at low temperature $T=0.02$. (b) AF and SC correlations at maximum distance for the model with eight impurities and without disorder (clean). The latter is the point $J=0.6$ of path 1. The disordered case corresponds to eight plaquettes on a 12×12 lattice. Typically, 5000 sweeps were used for thermalization and for measurements. With quenched disorder, many points were obtained after averaging over $N_{dis}=10$ disorder realizations. The results were found to mildly depend on the disorder configuration, thus, many results were obtained with a smaller N_{dis}.

III. MODEL II: LANDAU GINZBURG

The results reported thus far, based on Eq. (1), have already revealed interesting information, namely, the possible paths from AF to SC, and a proposed explanation of the glassy state as arising from the inevitable quenched disorder in the samples. However, the inhomogeneous nature of the clustered region suggests that percolative phenomena may be at work, and larger clusters are needed. To handle this issue, another model containing *only* classical DOF is proposed, with low-power interactions typical of Landau-Ginzburg (LG) approaches

$$H = r_1 \sum_{\mathbf{i}} |\Delta_{\mathbf{i}}|^2 + \frac{u_1}{2} \sum_{\mathbf{i}} |\Delta_{\mathbf{i}}|^4 + \sum_{\mathbf{i},\alpha} \rho_2(\mathbf{i},\alpha)\mathbf{S}_{\mathbf{i}} \cdot \mathbf{S}_{\mathbf{i}+\alpha} - \sum_{\mathbf{i},\alpha} \rho_1(\mathbf{i},\alpha)|\Delta_{\mathbf{i}}||\Delta_{\mathbf{i}+\alpha}|\cos(\Psi_{\mathbf{i}} - \Psi_{\mathbf{i}+\alpha}) + r_2 \sum_{\mathbf{i}} |\mathbf{S}_{\mathbf{i}}|^2 + \frac{u_2}{2} \sum_{\mathbf{i}} |\mathbf{S}_{\mathbf{i}}|^4 + u_{12} \sum_{\mathbf{i}} |\Delta_{\mathbf{i}}|^2 |\mathbf{S}_{\mathbf{i}}|^2. \quad (3)$$

The fields $\Delta_{\mathbf{i}}=|\Delta_{\mathbf{i}}|e^{i\Psi_{\mathbf{i}}}$ are complex numbers representing the SC order parameter. The classical spin at site $\mathbf{i}$ is $\mathbf{S}_{\mathbf{i}}=|\mathbf{S}_{\mathbf{i}}|[\sin(\theta_{\mathbf{i}})\cos(\phi_{\mathbf{i}}),\sin(\theta_{\mathbf{i}})\sin(\phi_{\mathbf{i}}),\cos(\theta_{\mathbf{i}})]$. $\rho_1(\mathbf{i},\alpha)=1-\rho_2(\mathbf{i},\alpha)$ is used as the analog of $V=1-J/2$ of the previous model to reduce the multiparameter character of the investigation, allowing an AF-SC interpolation changing just one parameter. α denotes the two directions $\hat{x}$ and $\hat{y}$ in two dimensions, and also $\hat{z}$ for multilayers. $\rho_2(\mathbf{i},\alpha)$ was chosen to be isotropic (i.e., α independent).

A. Basic properties

Clearly, the lowest-energy state for $\rho_2=0$ is a homogeneous SC state [if $\rho_1(\mathbf{i},\alpha)=\rho_1^0>0$]. When $\rho_1=0$ the lowest-

energy state is AF [if $\rho_2(\mathbf{i},\alpha)=\rho_2^0>0$]. In the clean limit, this model was already studied in the SO(5) context, where the reader is referred for further details. Our approach without disorder has similarities with SO(5) ideas[16] where the AF/SC competition, as the cause of the high-T_c phase diagram, was extensively discussed although nowhere in our investigations do we need to invoke a higher symmetry group. The relevance of tetracriticality in $La_2CuO_{4+\delta}$ has also been remarked by Demler *et al.*[25] and Sidis *et al.*[26] In the present work, disorder is introduced by adding a randomly selected bimodal contribution [i.e. $\rho_2(\mathbf{i},\alpha)=\rho_2^0\pm W$], where W is the disorder strength ($W=0$ is the clean limit). It is expected that other forms of disorder will lead to similar results.

B. Phase diagram

Monte Carlo results for Eq. (3) are in Fig. 4(a), for "weak" coupling $u_{12}=0.7$, which leads to tetracritical behavior. Both at $W=0$ and $W\neq 0$, the qualitative similarity with fermionic model results [Figs. 1(b) and 2(b)] is clear. Coexisting SC and AF clusters appear in MC snapshots (not shown). Then, both models share a similar phenomenology, and Eq. (3) can be studied on larger lattices. The only important difference between the two models is that Eq. (3) cannot lead to doped-undoped stripes, but the more general case Eq. (1) does. Figure 4(b) illustrates how the phase diagram in Fig. 4(a) was obtained. For completeness, note that by increasing the coupling u_{12} a first-order SC-AF transition can be obtained. However, the addition of disorder leads to a very similar phase diagram as in the case of $u_{12}=0.7$. This is shown in Fig. 4(c), and is the equivalent of Fig. 4(a) in the regime of "strong" coupling.

Some of the experiment predictions related to with our SC-AF clustered state are simple (the most elaborated ones are in Sec. IV). In most ways a very underdoped cuprate can be tested, there should be two components in the data. For instance, a typical photoemission spectra in our framework should have two clearly distinct coexisting signals. This result, which will be discussed in more detail in a future publication, is compatible with photoemission experiments for $x=0.03$ LSCO, which reveal spectral weight in the node direction of the *d*-wave superconductor even in the insulating glassy regime.[27] Nodal *d*-wave SC particles surviving to low x was observed in Ref. 28.

IV. COLOSSAL EFFECTS IN CUPRATES

One of the main results of these investigations is that the models studied here can present "colossal" effects, very similarly in spirit as it occurs in manganites. Consider a typical clustered state [Fig. 5(b)] found by MC simulations in the disordered region. This state has preformed local SC correlations—nanoscale regions having robust SC amplitudes within each region, but no SC phase coherence between different regions—rendering the state globally non-SC (the averaged correlation at the largest distances available C_{SC}^{max} is nearly vanishing). Let us now introduce an artificial SC "external field," which can be imagined as caused by the proximity of a layer with robust SC order (e.g., comprised of

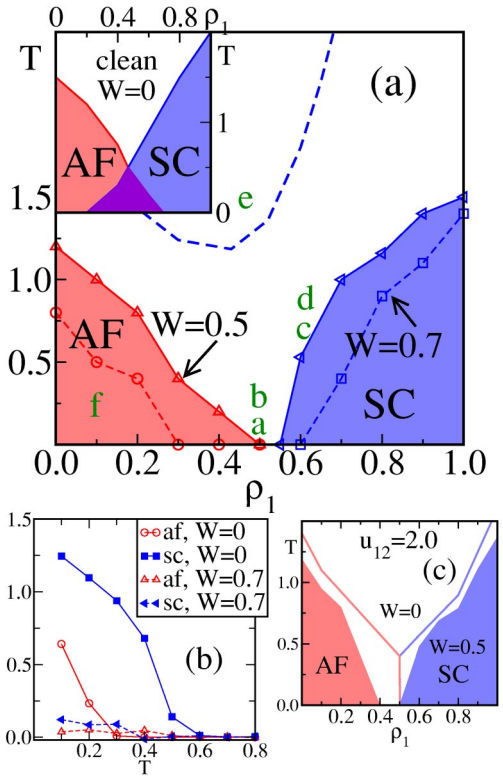

FIG. 4. (Color online) (a) MC phase diagram [for Eq. (3)] at $u_{12}=0.7$. Parameters are $r_1=-1$, $r_2=-0.85$, and $u_1=u_2=1$ but the conclusions are not dependent on coupling fine-tuning. Spin $C_{spin}(\mathbf{m})=(1/N)\Sigma_{\mathbf{i}}\langle \mathbf{S_i}\cdot\mathbf{S_{i+m}}\rangle$ and SC correlations $C_{SC}(\mathbf{m})=(1/N)\Sigma_{\mathbf{i}}|\Delta_{\mathbf{i}}||\Delta_{\mathbf{i+m}}|\cos(\Psi_{\mathbf{i}}-\Psi_{\mathbf{i+m}})$ were measured. The behavior of these functions at the largest (shortest) distance determine T_c and T_N (T^*) [same criteria as for Eq. (1)]. With disorder, the phase diagram (shown) has an intermediate "clustered" state with short-range order. T^* is also indicated (dashed line). Note the similarity with Fig. 2(b). Inset: results at $W=0$ showing tetracriticality [magenta (dark) indicates SC-AF coexistence]. (b) AF and SC correlations at maximum distance for the model Eq. (3) without and with disorder ($W=0.0$ and 0.7, respectively). $\rho_1=0.5$ and $u_{12}=0.7$ were used, using a 24×24 lattice. Typically, for the LG model 25 000 sweeps were used for thermalization and measurements. (c) MC phase diagram of model Eq. (3) at $u_{12}=2$. The clean case ($W=0$, solid lines) is bicritical-like, but with disorder $W=0.5$ a clustered region between SC and AF opens as well.

a higher-T_c material). In practice, this is achieved in the calculations by introducing a term $|\Delta_{SC}^{ext}|\Sigma_{\mathbf{i}}\rho_1(\mathbf{i},\hat{z})|\Delta_{\mathbf{i}}|\cos(\Psi_{\mathbf{i}})$, where Δ_{SC}^{ext} acts as an external field for SC. The dependence of C_{SC}^{max} with Δ_{SC}^{ext} is simply remarkable [Fig. 5(a)]. While at points *e* and *f*, located far from the SC region in Fig. 4(a), the dependence is the expected one for a featureless state (linear): the behavior closer to SC and small temperatures is highly nonlinear and unexpected. For example, at point *a*, C_{SC}^{max} versus Δ_{SC}^{ext} has a slope (at $\Delta_{SC}^{ext}=0.02$), which is $\sim$250 *times larger* than at *e* ($\sim$13 times larger than at $W=0$, same T, ρ_2, and u_{12}).

The reason for this anomalous behavior is the clustered nature of the states. This is shown in the state in Fig. 5(c), contrasted with (b), where a relatively small field—in the natural units of the model—nevertheless, led to a quick

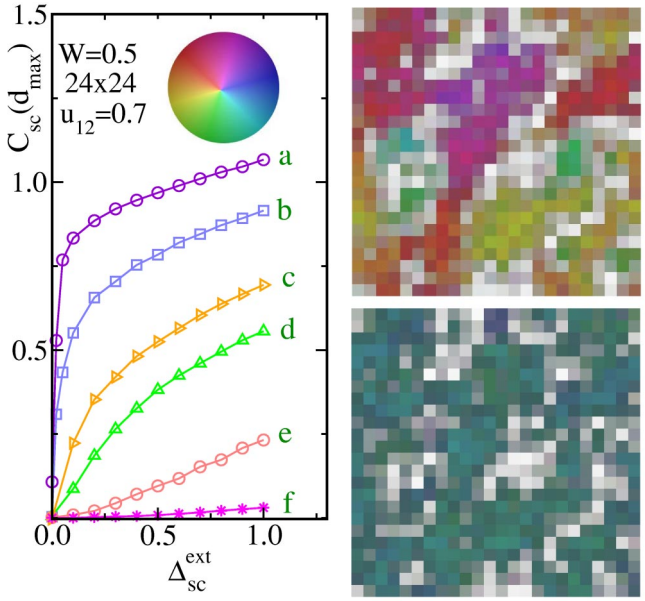

FIG. 5. (Color online) Left: C_{SC}^{max} versus Δ_{SC}^{ext} (see text) on a 24×24 lattice, with $u_{12}=0.7$ and $W=0.5$, at the five points *a*-*f* indicated in Fig. 4(a). A "colossal" effect is observed in *a* and *b* where the $\Delta_{SC}^{ext}=0$ state is "clustered." A much milder (linear) effect occurs far from the SC phase (*e* and *f*). MC snapshots are shown at $\Delta_{SC}^{ext}=0.0$ (right, top) and $\Delta_{SC}^{ext}=0.2$ (right, bottom), both at $T=0.1$ and $\rho_2=0.5$, using the same quenched-disorder configuration. The color convention is explained in the circle [colors indicate the SC phase, while intensities are proportional to $\mathrm{Re}(\Delta_i)$]. The AF order parameter is not shown. The multiple-color nature of the upper snapshot, reflects a SC phase randomly distributed (i.e., an overall non-SC state). However, a small external field rapidly aligns those phases, leading to a coherent state (*bottom*).

alignment of SC phases, producing a globally SC state, as can be inferred from the uniform color of the picture. *Having preformed SC puddles vastly increases the SC susceptibility*. Because Fig. 5(a) was obtained in a trilayer geometry, it is tempting to speculate that the proximity of SC layers to a non-SC but clustered state, can naturally lead to a GPE over long distances, as observed experimentally in a similar geometry.[1–3]

V. DEPENDENCE OF T_c WITH THE NUMBER OF LAYERS

The nanoscale clusters also lead to a proposal for explaining the *rapid* increase of T_c with the number of Cu-oxide layers N_ℓ, found experimentally, at least up to three layers. In this effort, the MC phase diagrams of single-, bi-, and trilayer systems described by Eq. (3), with and without disorder, were calculated using exactly the same parameters (besides a coupling $\rho_2(\mathbf{i},\hat{z})$, equal to those along $\hat{x}$ and $\hat{y}$, to connect the layers). It was clearly observed that *the single layer has a substantially lower T_c than the bilayer*. This can be understood in part from the obvious critical fluctuations that are stronger in two than three dimensions. But even more important, cluster percolation at $W\neq0$ is more difficult in two than three dimensions (since otherwise two-

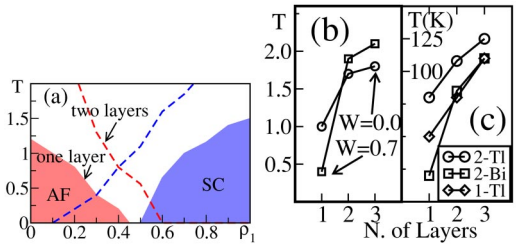

FIG. 6. (Color online) (a) MC phase diagram [for Eq. (3)] at $u_{12}=0.7$. Parameters are $r_1=-1$, $r_2=-0.85$, $u_1=u_2=1$, and $W=0.5$ with one layer (solid colors) and two layers (dashed line). The addition of an extra layer increases the critical temperature of the superconductor as well as the Néel temperature. (b) T_c vs N_ℓ for $u_{12}=0.7$, $\rho_2=0.3$, $W=0.7$, and $24^2\times N_l$ clusters. Shown are results with and without disorder. (c) The experimental T_c (in K) is shown for three HTS families, as indicated, up to three layers (data from Ref. 29).

dimensional (2D) disconnected clusters may become linked through an interpolating cluster in the adjacent layer). Then, in the phenomenological approach presented here it is natural that T_c increases fast with N_ℓ when changing from 1 to 2 layers as shown in Fig. 6(a). This concept is even *quantitative*—up to a scale—considering the similar shape of T_c versus N_ℓ found both in the MC simulation and in experiments [see Figs. 6(b) and 6(c)]. Note that the subsequent decrease of T_c for 4 or more layers observed experimentally could be caused by inhomogeneous doping, beyond our model). Our MC results suggest that the large variations of T_c's known to occur in single-layer cuprates can be attributed to the sensitivity of 2D systems to disorder. As N_ℓ increases [the system becomes more three dimensional (3D)], the influence of disorder *decreases*, both in experiments[30] and simulations.

VI. CONCLUSIONS

Summarizing, here simple phenomenological models for phase competition showed that, depending on details, different cuprates could have stripes, local coexistence, first-order transitions, or a glassy clustered state interpolating between AF and SC phases. Figure 7 illustrates our proposed possibilities. In Cu-oxides where the glass state is realized, namely, where SC puddles are present, this study revealed the possibility of colossal effects. A schematic representation of the proposed glassy state with colossal effects is shown in Fig. 8. This proposal could provide rationalization of recent results in trilayer thin-film geometries.[1–3]

After submission of this work, we learned of interesting experimental efforts that complement the discussion presented here: (i) In Ref. 31, further evidence of an anomalous proximity effect in the cuprates is presented. These results add to those of Ref. 1–3, showing that the anomalous effects are real. (ii) In Refs. 32 and 33, the phase diagram of yttrium barium copper oxide (YBCO) was recently investigated in the presence of Ca doping. Among many results, it was shown that a glassy state is generated between the AF and SC states in Ca-doped YBCO, with a phase diagram very

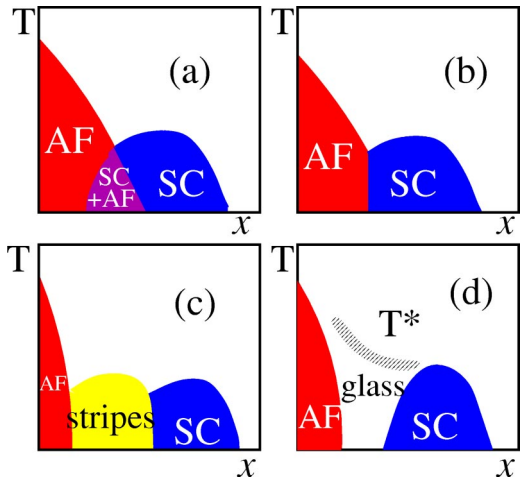

FIG. 7. (Color online) Schematic representation of the phase diagrams that our models show in the clean (a)–(c) and dirty (d) limits. The theory discussed in this paper shows the possible appearance of regions with *local* coexistence of AF and SC (a), or a first-order transition separating AF from SC (b) with the first-order character of the transition possibly continuing in the AF-disordered and SC-disordered transitions, or an intermediate striped regime (c). Possibilities (a) and (b) have already been discussed in Ref. 16, although here we do not invoke a higher-symmetry group, such as SO(5). The main result contained in this figure is the proposed phase diagram in the presence of quenched disorder (d). Shown are the glassy region, proposed to be a mixture of SC and AF clusters, and the T^*, where local order starts upon cooling. This phase diagram has similarities to those proposed before for manganites,[4,5] and certainly it is in excellent agreement with the experimental phase diagram of LSCO.

similar to that in LSCO and our Fig. 7(d). This result suggests that *Ca-undoped* YBCO may have either a region of local coexistence of SC and AF or a first-order transition separating them [as in Figs. 7(a) and 7(b)], and only with the help of extra quenched disorder is a glassy state generated. Then, the generic phase diagram of the cuprates, which usually is considered to be that of LSCO, may not be as universal as previously believed, as discussed in this paper. Our study showing that bilayered systems are more stable than single layers with respect to disorder is also compatible with the experiment results of Refs. 32 and 33, namely, the one-

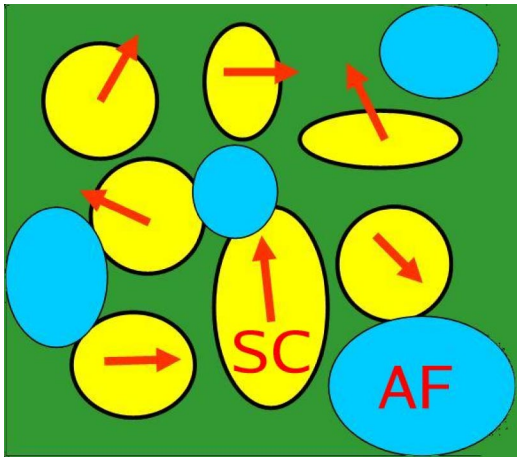

FIG. 8. (Color online) Schematic representation of the glassy state that separates the SC and AF regions. The arrow indicates the phase of the SC order parameter.

layer material is more likely to have a glassy state between AF and SC than two- or higher-layer materials. (iii) Our effort has already induced interesting theoretical work[34] in the context of *J-U* models. (iv) Theoretical work[35] closely related to our proposed glassy state in Fig. 7 has addressed inhomogeneous Josephson phases near the superconductor-insulator transition. (v) Recent neutron- and Raman-scattering investigations applied to $La_2CuO_{4.05}$ have shown the coexistence of SC and AF phases in this compound.[36] (vi) Finally, our results have similarities with those recently discussed in the context of *Bose metals* as well.[37]

The study also provided predictions for photoemission experiments (to be discussed elsewhere) and a simple explanation for the T_c increase with N_ℓ (another explanation can be found in Ref. 38). Clustered states are crucial in manganites and other compounds,[39] and this analysis predicts its potential relevance in HTS materials as well.

ACKNOWLEDGMENTS

This work was financially supported by NSF Grant No. DMR 0443144. Conversations with S. L. Cooper, J. Tranquada, S. Sachdev, M. Greven, S. Chakravarty, and S.C. Zhang are gratefully acknowledged. Most calculations were performed on the CMT computer cluster at the NHMFL.

[1] I. Bozovic, G. Logvenov, M. A. J. Verhoeven, P. Caputo, E. Goldobin, and M. Beasley, Phys. Rev. Lett. **93**, 157002 (2004).
[2] R. S. Decca, H. D. Drew, E. Osquiguil, B. Maiorov, and J. Guimpel, Phys. Rev. Lett. **85**, 3708 (2000).
[3] J. Quintanilla, K. Capelle, and L. Oliveira, Phys. Rev. Lett. **90**, 089703 (2003).
[4] *Nanoscale Phase Separation and Colossal Magnetoresistance*, edited by E. Dagotto (Springer-Verlag, Berlin, 2002).
[5] E. Dagotto, T. Hotta, and A. Moreo, Phys. Rep. **344**, 1 (2001).
[6] Y. Tokura and N. Nagaosa, Science **288**, 462 (2000).
[7] J. M. Tranquada, B. J. Sternlieb, J. D. Axe, Y. Nakamura, and S. Uchida, Nature (London) **375**, 561 (1995).
[8] V. Emery, S. A. Kivelson, and H. Q. Lin, Phys. Rev. Lett. **64**, 475 (1990).
[9] K. Lang, V. Madhavan, J. E. Hoffman, E. W. Hudson, H. Eisaki, S. Uchida, and J. C. Davis, Nature (London) **415**, 412 (2002).
[10] Y. Kohsaka, K. Iwaya, S. Satow, T. Hanaguri, M. Azuma, M. Takano, and H. Takagi, Phys. Rev. Lett. **93**, 097004 (2004).
[11] S. Sorella, G. B. Martins, F. Becca, C. Gazza, L. Capriotti, A. Parola, and E. Dagotto, Phys. Rev. Lett. **88**, 117002 (2002).
[12] S. White and D. J. Scalapino, Phys. Rev. Lett. **80**, 1272 (1998).
[13] W. A. Atkinson, P. J. Hirschfeld, and L. Zhu, Phys. Rev. B **68**,

054501 (2003).
[14] A. Ghosal, C. Kallin, and A. J. Berlinsky, Phys. Rev. B **66**, 214502 (2002).
[15] M. Ichioka and K. Machida, J. Photogr. Sci. **68**, 4020 (1999).
[16] S. Zhang, Science **275**, 1089 (1997).
[17] M. Moraghebi, S. Yunoki, and A. Moreo, Phys. Rev. Lett. **88**, 187001 (2002).
[18] J. M. T. Axel, D. Axel, N. Ichikawa, A. R. Moodenbaugh, Y. Nakamura, and S. Uchida, Phys. Rev. Lett. **78**, 338 (1997).
[19] D. Poilblanc and T. M. Rice, Phys. Rev. B **39**, 9749 (1989).
[20] J. Zaanen and O. Gunnarsson, Phys. Rev. B **40**, 7391 (1989).
[21] V. Emery and S. Kivelson, Physica C **209**, 597 (1993).
[22] V. Emery and S. Kivelson, Physica C **235**, 189 (1994).
[23] H.-D. Chen, S. Capponi, F. Alet, and S.-C. Zhang (2003), cond-mat/0312660 (unpublished).
[24] X. Zhou, T. Yoshida, S. A. Kellar, P. V. Bogdanov, E. D. Lu, A. Lanzara, M. Nakamura, T. Noda, T. Kakeshita, H. Eisaki, S. Uchida, A. Fujimori, Z. Hussain, and Z.-X. Shen, Phys. Rev. Lett. **86**, 5578 (2001).
[25] E. Demler, S. Sachdev, and Y. Zhang, Phys. Rev. Lett. **87**, 067202 (2001).
[26] Y. Sidis, C. Ulrich, P. Bourges, C. Bernhard, C. Niedermayer, L. P. Regnault, N. H. Andersen, and B. Keimer, Phys. Rev. Lett. **86**, 4100 (2001).
[27] T. Yoshida, X. J. Zhou, T. Sasagawa, W. L. Yang, P. V. Bogdanov, A. Lanzara, Z. Hussain, T. Mizokawa, A. Fujimori, H. Eisaki, Z.-X. Shen, T. Kakeshita, S. Uchida, Phys. Rev. Lett. **91**, 027001 (2003).
[28] A. Hossein, D. Broun, D. Sheehy, T. Davis, M. Franz, R. Liang, W. Hardy, and D. Bonn, cond-mat/0312542 (unpublished).
[29] G. Burns, *High-Temperature Superconductivity: An Introduction* (Academic Press, Inc., San Diego, 1992).
[30] H. Eisaki, N. Kaneko, D. Feng, A. Damascelli, P. Mang, K. Shen, Z.-X. Shen, and M. Greven, cond-mat/0312570 (unpublished).
[31] I. Asulin, A. Sharoni, O. Yulli, G. Koren, and O. Millo, Phys. Rev. Lett. **93**, 157001 (2004).
[32] S. Sanna, G. Allodi, G. Concas, and R. D. Renzi (unpublished).
[33] S. Sanna, G. Allodi, G. Concas, A. Hillier, and R. D. Renzi, cond-mat/0403608 (unpublished).
[34] L. Arrachea and D. Zanchi, cond-mat/0409141 (unpublished).
[35] J. Tu, M. Strongin, and Y. Imry, report, 2004 (unpublished).
[36] V. Gnezdilov, Y. Pashkevich, J. Tranquada, P. Lemmens, G. Güntherodt, A. Yeremenko, S. Barilo, S. Shiryaev, L. Kurnevich, and P. Gehring, cond-mat/0403340 (unpublished).
[37] P. Phillips and D. Dalidovich, Science **302**, 243 (2003).
[38] S. Chakravarty, H.-Y. Kee, and K. Völker, Nature (London) **428**, 53 (2004).
[39] H. Rho, C. S. Snow, S. L. Cooper, Z. Fisk, A. Comment, and J.-P. Ansermet, Phys. Rev. Lett. **88**, 127401 (2002).